

# AN AUGMENTED THREE-ANTENNA PROBE CALIBRATION TECHNIQUE FOR MEASURING PROBE INSERTION PHASE

Aksel Frandsen<sup>1</sup>, Doren W. Hess<sup>2</sup>, Sergey Pivnenko<sup>3</sup>, and Olav Breinbjerg<sup>3</sup>

<sup>1</sup>TICRA  
Læderstræde 34,  
DK-1201 Copenhagen K, Denmark  
[aksel@ticra.com](mailto:aksel@ticra.com)

<sup>2</sup>MI Technologies  
4500 River Green Parkway,  
Duluth, Georgia 30096, USA  
[dhess@mi-technologies.com](mailto:dhess@mi-technologies.com)

<sup>3</sup>Electromagnetic systems, Ørsted-DTU,  
Technical University of Denmark,  
DK-2800 Kgs. Lyngby, Denmark  
[sp@oersted.dtu.dk](mailto:sp@oersted.dtu.dk), [ob@oersted.dtu.dk](mailto:ob@oersted.dtu.dk)

## Abstract

**Probe calibration is a prerequisite for performing high accuracy near-field antenna measurements. One convenient technique that has been used with confidence for years consists of using two auxiliary antennas in conjunction with the probe-to-be-calibrated. Inherent to this technique is a calibration of all three antennas. So far the technique has mostly been applied to calibrate for polarization and gain characteristics. It is demonstrated how the technique can be extended to also measure an antenna's phase-versus-frequency characteristic.**

Key words: Probe calibration, three-antenna measurements.

## 1. Introduction

Calibration of a probe for near-field scanning involves determination of the probe's amplitude and phase radiation patterns, together with a determination of its gain, its polarization characteristics, its port reflection coefficient(s), and, if the probe is dual polarized, the channel balance, i.e. the amplitude and phase difference between its two ports [1].

The calibration measurements shall be performed across the frequency band for which the probe is intended. Whereas the measurement of the probe's radiation patterns involves the use of one auxiliary utility antenna, the determination of the probe's polarization characteristics and gain is usually accomplished through a conventional three-antenna measurement procedure [2], in which the probe and two auxiliary utility antennas form a set of three unknown antennas. Measuring in turn the three possible antenna pairs in front of each other, one on the antenna tower, the other

on the probe tower, allows one to determine the required calibration data for each antenna in the set. Alternatively, the probe's gain may be determined through a near-field substitution technique [1].

For the vast majority of cases, these calibration data will be sufficient to characterize the probe. However, for some applications it is desired to also determine the probe's *phase-versus-frequency* characteristics, being here defined as the phase delay from the reference plane at the probe's port to the aperture plane of the probe, as a function of frequency. In line with the meaning of the term *insertion loss*, it would seem natural to coin this phase delay the *insertion phase* of the probe.

This characteristic of the probe may be measured by *augmenting* the conventional three-antenna probe calibration procedure to include also the measurement of the on-axis insertion phase of each pair, which in turn results in the determination of the individual phase-versus-frequency characteristics for each member in the set. The augmented measurement thus complements the conventional probe calibration, and allows the determination of the phase of the probe's spherical modal scattering coefficients,  $T_{\sigma\mu\nu}$  and  $R_{\sigma\mu\nu}$  for transmitting and receiving, respectively [1].

## 2. Measurement Set-up

The Antenna-Under-Test (AUT) is an S-band MI Technologies Series 31 Dual-Ported Orthomode Probe, Model 31-2.6, equipped with a polarization switch box, and mounted on a metal bracket, to which a rectangular plate of microwave absorber can be affixed. This whole structure is referred to as a Dual-Ported Probe Assembly (DPPA),

shown in Figure 1 mounted on the antenna tower at the calibration range.

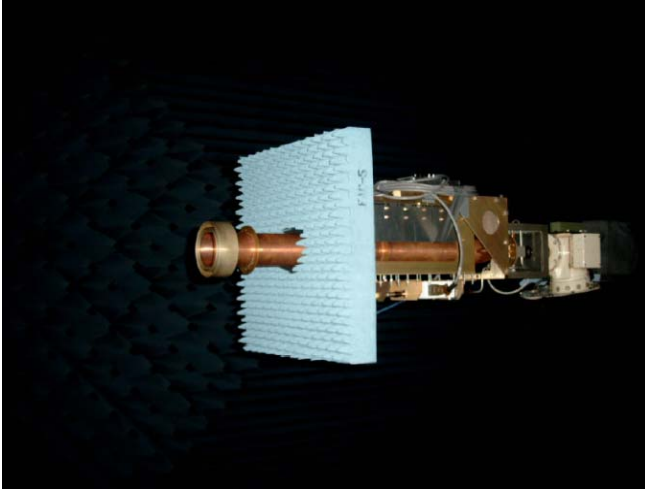


**Figure 1. Dual-Ported Probe Assembly on antenna tower.**

The measurement set-up at the DTU-ESA Spherical Near-Field Antenna Test Facility is shown schematically in Figure 2 below.

The Facility's anechoic chamber, 17 m long, 12 m wide and 10 m high, is equipped with a Scientific-Atlanta Model 2180 Signal Source and a Scientific-Atlanta Model 1795 Microwave Receiver. The antenna tower is an elevation-over-azimuth spherical scanner, providing two axes of rotation : a vertical axis ( $\theta$ -axis), and a horizontal axis ( $\phi$ -axis), allowing for full sphere measurements at a constant distance using the probe on the probe tower. Detailed descriptions of the Facility may be found in [3-4].

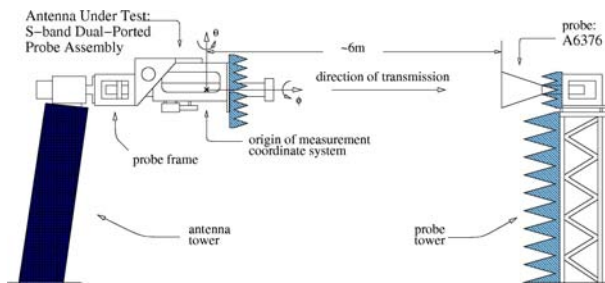


**Figure 2. Measurement set-up.**

### 3. Measurement Procedure

The purpose of the measurement is to determine the insertion phase of the DPPA versus frequency. This may be accomplished by a three-antenna measurement procedure, where the DPPA is one of a set of three antennas, each considered to be unknown. Three pairs of antennas can then

be measured in front of each other, and the final result will be a determination of the relative insertion phase versus frequency for each of the three antennas. With reference to Figure 2, we have to the left the Antenna Tower (AT), and to the right the Probe Tower (PT). For the present phase measurements, the distance between any pair of antennas is measured from aperture-plane to aperture-plane. The insertion phase for any antenna in the set is then the total phase delay from that antenna's input connector to its aperture plane.

The DPPA is equipped with a control box to allow switching between its two ports, 1 and 2, corresponding to nominally X-polarized and Y-polarized ports, respectively. The phase insertion for both ports shall be determined.

The two auxiliary utility antennas in the three-antenna measurement procedure consist of two 'identical' Scientific-Atlanta Series 12 Standard Gain Horns (SGH), Model 12-2.6, denoted A6375 and A6376. The 3 pairs to be measured are then as follows :

| Antenna pair | On AT | On PT | Inter-aperture distance |
|--------------|-------|-------|-------------------------|
| 1-2          | DPPA  | A6375 | 5323.0 mm               |
| 1-3          | DPPA  | A6376 | 5323.0 mm               |
| 2-3          | A6375 | A6376 | 5882.5 mm               |

**Table 1. Antenna combinations for three-antenna measurements.**

Taking the total measured phase delay to be that of the phase delays in the antennas on the AT and on the PT, plus the phase delay in the free space between the antenna apertures, one can write equations for each of the measured phases,  $\Phi_{12}^{meas}$ ,  $\Phi_{13}^{meas}$ , and  $\Phi_{23}^{meas}$ , in these combinations as follows

$$1-2 : \quad \Phi_{12}^{meas} = \Phi_1 + \Phi_2 + \Phi_{12}^{fsp}$$

$$1-3 : \quad \Phi_{13}^{meas} = \Phi_1 + \Phi_3 + \Phi_{13}^{fsp}$$

$$2-3 : \quad \Phi_{23}^{meas} = \Phi_2 + \Phi_3 + \Phi_{23}^{fsp}$$

where

$\Phi_1$  is the phase delay in the DPPA,

$\Phi_2$  is the phase delay in the SGH A6375,

$\Phi_3$  is the phase delay in the SGH A6376

and  $\Phi_{12}^{fsp}$ ,  $\Phi_{13}^{fsp}$ ,  $\Phi_{23}^{fsp}$  are the free space phase delays between the apertures of the antennas on the AT and PT. Since the inter-aperture distances are known (cf. Table 1), the phase delays may be calculated assuming far field

propagation conditions. However, since the far fields of the individual antennas in Table 1 are determined in the conventional calibration procedure from a spherical near-field to far-field transformation using SNIFTD, we do not have to rely on far-field propagation conditions. From the transformations we automatically obtain the corresponding Spherical Wave Expansions, and then we evaluate these expansions at the actual near-field position of the antenna on the Probe Tower, arriving at a more accurate value for the phase delay between the antennas.

The three equations above may be solved for the phase delays in each of the antennas. In doing this, one must carefully keep track of the phase cycles. This may be accomplished by first 'rectifying' the measured phases,  $\Phi_{12}^{meas}$ ,  $\Phi_{13}^{meas}$ ,  $\Phi_{23}^{meas}$ , i.e. from the measured phase data taken within the  $\pm 180^\circ$  regime one creates continuous phase delay functions.

The solutions then read :

$$\Phi_1 = [\Phi_{12}^{meas} + \Phi_{13}^{meas} - \Phi_{23}^{meas} - \Phi_{12}^{fsp} - \Phi_{13}^{fsp} + \Phi_{23}^{fsp}] / 2$$

$$\Phi_2 = [\Phi_{12}^{meas} - \Phi_{13}^{meas} + \Phi_{23}^{meas} - \Phi_{12}^{fsp} + \Phi_{13}^{fsp} - \Phi_{23}^{fsp}] / 2$$

$$\Phi_3 = [-\Phi_{12}^{meas} + \Phi_{13}^{meas} + \Phi_{23}^{meas} + \Phi_{12}^{fsp} - \Phi_{13}^{fsp} - \Phi_{23}^{fsp}] / 2$$

Finally, to provide a measurement reference for the measured phases,  $\Phi_{12}^{meas}$ ,  $\Phi_{13}^{meas}$ ,  $\Phi_{23}^{meas}$ , one needs to 'short-circuit' the range. This is carried out by disconnecting the antennas on the AT and the PT from the respective tower cables, and then connecting a long cable directly between the AT and the PT cable connectors. A Semflex LA290, phase stable cable, ~10 meters long, was employed to obtain this reference. The cable itself was also measured on a calibrated HP8510 Vector Network Analyzer to obtain the phase of the transmission coefficients  $S_{12}$  and  $S_{21}$ . In all measurements with this cable, two 20 dB HP attenuators were included as a part of the cable.

#### 4. Measurement Results

The DPPA shall be used in the frequency band from 2.5 GHz to 3.5 GHz. The conventional calibration for radiation pattern, polarization, gain and channel balance was carried out with a frequency increment of 50 MHz, i.e. for a total of 21 frequencies.

With a measurement distance slightly less than 6 meters, the overall free space phase delay between the apertures of the two antennas from 2.5 GHz to 3.5 GHz amounts to ~7100 electrical degrees, or almost 20 complete phase cycles. To this must be added the phase delays in the antennas themselves. Assuming simple  $TE_{11}$  mode propagation, the longest propagation path in the DPPA

waveguide has a phase delay of ~1900 degrees. Semi-rigid cables, attenuators and the switch box were estimated to contribute another phase delay of ~1500 degrees. For the SGH, which is rather short, a delay of less than 1000 degrees is expected. Adding all up then, we arrive at a total rough estimate of 11000 to 11500 electrical degrees for the total phase delay from the antenna connector on the AT to the antenna connector on the PT, or ~32 phase cycles.

In order not to 'lose' phase cycles, the samples in frequency must be fairly closely spaced. Simulations have shown that 3 samples per cycle are sufficient, and hence a frequency interval of 10 MHz were chosen, making a total of 101 samples in the 1000 MHz frequency interval, This is in contrast to the 50 MHz interval for the conventional calibration.

At each measurement frequency a total of 2048 samples of the signal were used to generate the final 'read-out'. This was carried out 5 times, followed by an averaging of these data. Figures 3 and 4 show examples of these averaged, measured phase data for the three-antenna measurements defined in Table 1 above. The measurement for the 'short-circuited' range with the phase stable cable between the two towers is shown in Figure 5. The right scales on the plots show the standard deviations of the measured phase data, which in all cases are less than  $0.02^\circ$ .

The phase stable cable was then measured on an HP8510 Vector Network Analyzer. The phases of the transmission coefficients  $S_{21}$  and  $S_{12}$  are shown in Figure 6, together with the difference between the two sets of measurements. The average difference is less than  $1^\circ$ . The two sets were averaged for their use in the further processing.

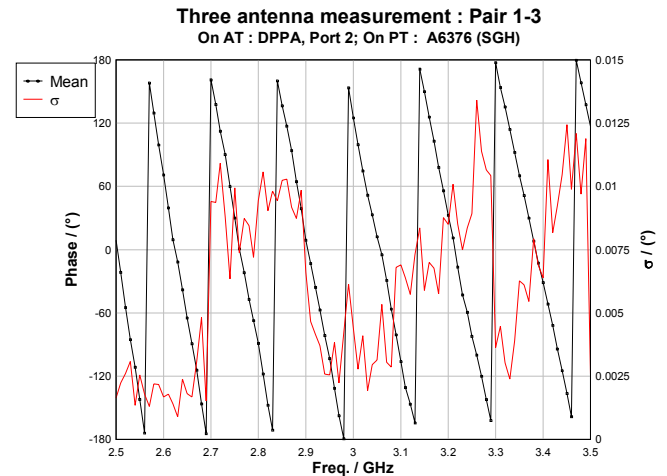


Figure 3. Measured phase for antenna pair 1-3 : DPPA Port 2 and A6376 (SGH)

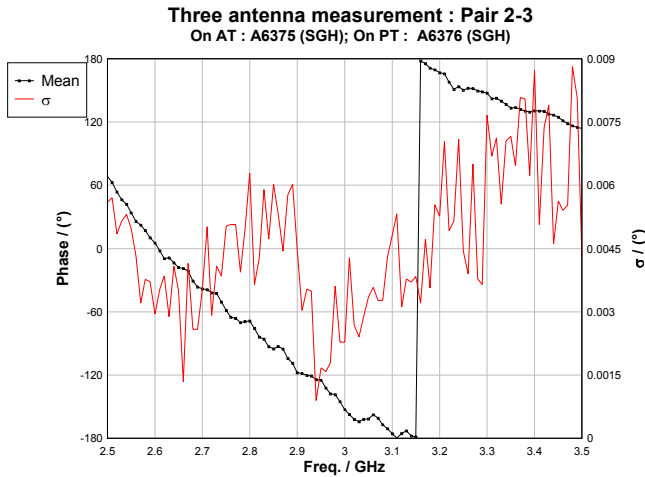


Figure 4. Measured phase for antenna pair 2-3 : A6375 (SGH) and A6376 (SGH)

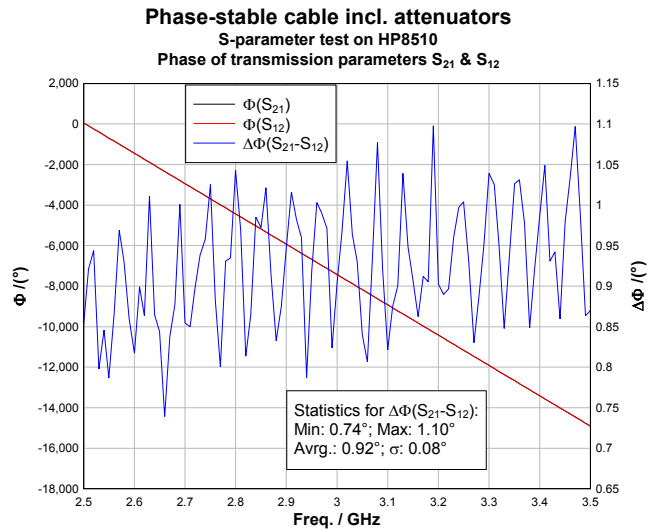


Figure 6. Measured phase of transmission coefficients  $S_{21}$  and  $S_{12}$  and their difference for long phase stable cable.

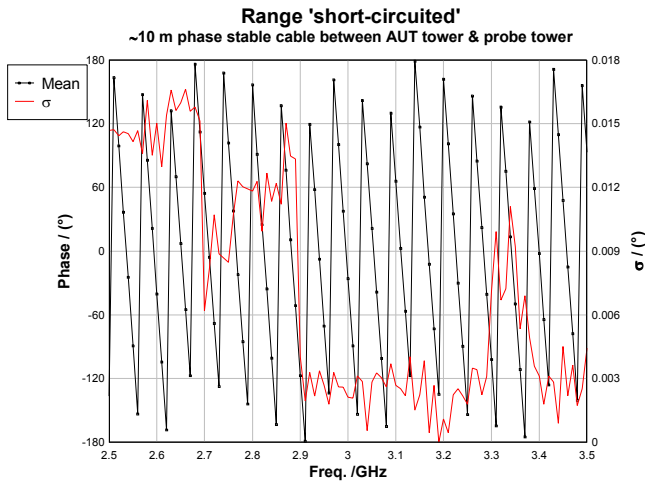
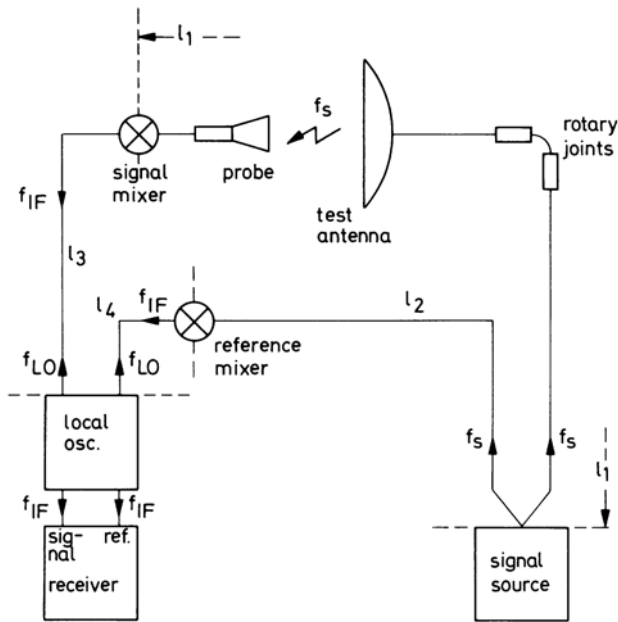


Figure 5. Measured phase for long phase stable cable between the towers.

A closer look at the plots of the measured phases (Figures 3 and 4) reveals that the expected number of phase cycles is not observed. For the free space propagation between the two antenna apertures, 18 to 20 phase cycles should be present. Figure 7 below [1, p.177] explains the cause of the 'missing' cycles : To make the phase measurements least sensitive to changes and variations, the phase delays in the two legs  $l_1$  and  $l_2$  should be equal. This is achieved by employing a long semi-rigid cable from the transmitter to the receiver, which – so to speak - 'counter-balances' the free-space phase delay. The reference phase, to which all the measured phases above shall be referred, is then obtained by the difference between the phase measured on the HP8510 VNA, and the phase measured when the cable was connected between the two towers.

Before proceeding to finally solve for the insertion phases of each of the antennas, we need to calculate the phase delay in free space between the two antenna apertures. If far-field propagation conditions can be assumed, this delay is simply given by the usual phase factor of  $(-2\pi R/\lambda)$ ,  $R$  being the inter-aperture distance (cf. Table 1) and  $\lambda$  the wavelength.



**Figure 7. Schematics of RF system at the DTU-ESA Spherical Near-Field Antenna Test Facility**

However, since the far fields of the individual antennas are at our disposal from the conventional calibration measurements, we can make Spherical Wave Expansions of these far fields, and subsequently evaluate these expansions at the actual near-field distance. Since the far fields are only available for each 50 MHz, while the phase measurements are performed at 10 MHz intervals, we interpolate from the 50 MHz to the 10 MHz. This is done in the following way : The near-field phase calculated from the 50 MHz-spaced data is compared with the far-field phase, and the difference between the two is found. We then interpolate in the difference to obtain intermediate values at 10 MHz intervals. These interpolated values of the difference are then added to the far-field phase to give the near-field phase at 10 MHz intervals.

For the DPPA the difference between the far-field propagation assumption and the phase of the actual near field at the position of the antenna on the Probe Tower amounts to less than  $\sim 1^\circ$ . For the SGH, however, the difference is larger, amounting to  $\sim 3^\circ$ , in accordance with the higher directivity of the SGH, and hence its larger far field distance.

Based on the measured data and the corrections described above we have solved for the insertion phases for the individual antennas, i.e. the DPPA-Port 1, the DPPA-Port 2, the SA12-2.6 SGH # A6375, and the SA12-2.6 SGH # A6376. Figures 8 and 9 show the insertion phases for the two ports of the DPPA, normalized to  $0^\circ$  insertion phase for Port 1 of the DPPA at a frequency of 3.0 GHz. The plots present both the solution obtained for far-field and

near-field propagation assumptions, as well as the difference between the two.

The solutions for the two SA12-2.6 SGHs are shown in Figure 10, where also the difference between them is shown. It is seen that their insertion phases are practically identical. These were not normalized as was done for the DPPA.

Finally, the difference between the insertion phases for Port 1 (X) and Port 2 (Y) of the DPPA is calculated. This directly gives the phase of the channel balance,  $A_{x/y}$ , which has been measured independently, when the DPPA was calibrated for pattern, polarization and gain. Hence this comparison is a good test of the accuracy of both measurements. This is shown in Figure 11. The differences between the two sets of measurements are immaterial, and the agreement is excellent.

The phase stability and accuracy of the system is high, and the dominant source of error is in the measurement of distance. This can be measured within  $\pm 1$  mm, which at 3 GHz amounts to  $\pm 3.6^\circ$ . However, the distance term only enters into the solution with half weight, so that this term effectively contributes only  $\pm 1.8^\circ$ . Hence the overall accuracy is estimated to be well within the  $\pm 3.0^\circ$  requirement.

## 5. Conclusions

An augmented three-antenna measurement technique that complements the conventional probe calibration technique has been proposed and demonstrated for measuring the insertion phase of a near-field measuring probe. Excellent agreement with independently measured data has been obtained.

## References

- [1] Hansen, J.E. (ed.), "Spherical Near-Field Antenna Measurements", *Peter Peregrinus, Ltd.*, on behalf of IEE, London, 1988.
- [2] "IEEE Standard Test Procedures for Antennas", IEEE STD 149-179, *IEEE Inc.*, New York, December 1979.
- [3] Dich, M., Gram, H.E., "System Design and Measurement Procedures in Spherical Near Field Antenna Testing", *Proceedings of the 18<sup>th</sup> annual AMTA Meeting and Symposium*, pp. 342-347, Seattle, WA, USA, 1996.
- [4] Dich, M., Gram, H.E., "Alignment Errors and Standard Gain Horn Calibrations", *Proceedings of the 19<sup>th</sup> annual AMTA Meeting and Symposium*, pp. 425-430, Boston, MA, USA, 1997.

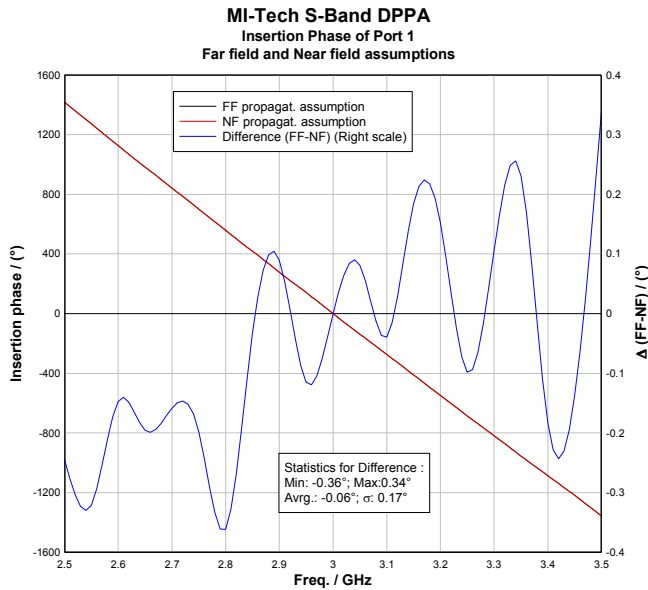


**Figure 8. Insertion phase for DPPA Port 1. Near- and far-field propagation and difference. Normalized to 0° at 3.0 GHz**

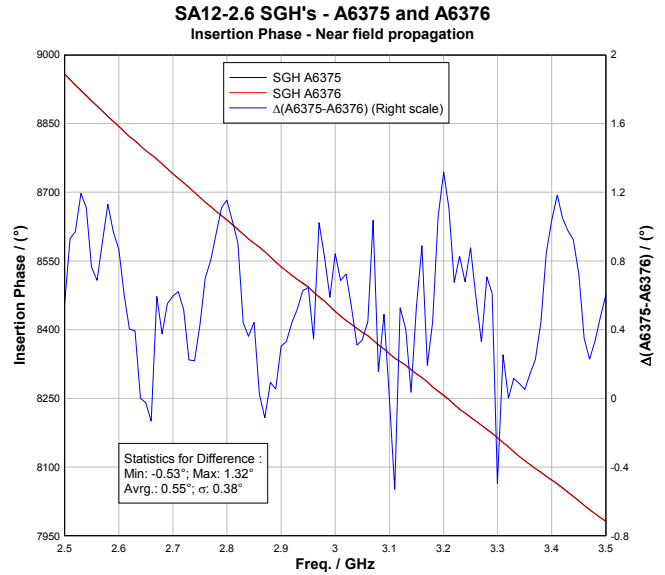


**Figure 10. Insertion phase for SGHs. Near-field propagation and difference between the two. No normalization.**

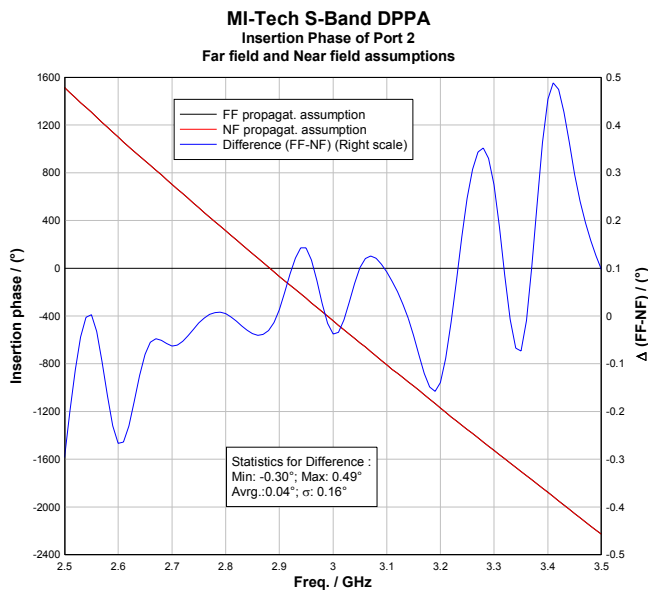


**Figure 9. Insertion phase for DPPA Port 2. Near- and far-field propagation and difference Normalized to 0° for Port 1 at 3.0 GHz**

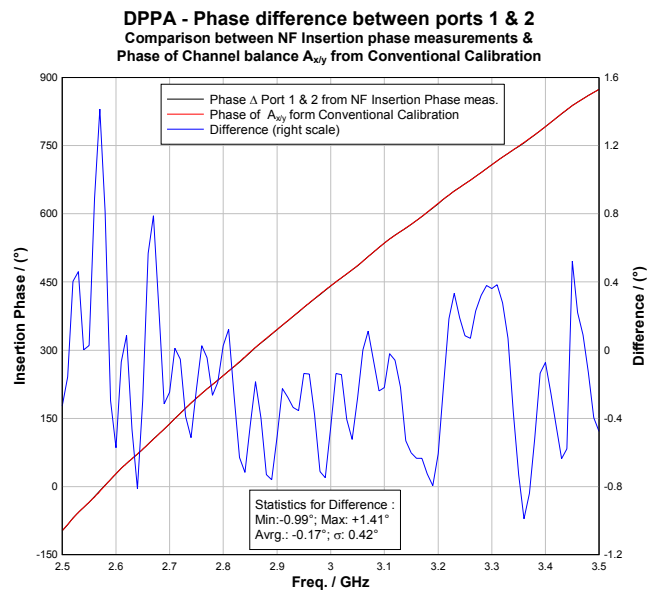


**Figure 11. Phase of Channel Balance. Comparison between near-field insertion phase and conventional calibration measurements.**